

# Reproducing and updating results from *Uncovering disease-disease relationships through the incomplete interactome*

Robin Petit<sup>1</sup> and Tom Lenaerts<sup>1</sup>

<sup>1</sup>Université Libre de Bruxelles

## Abstract

This paper intends to reproduce some of the results of the article *Uncovering disease-disease relationships through the incomplete interactome* (Menche et al., 2015) and check the robustness of the procedure by comparing the results obtained with the data of the original paper with the results obtained with updated datasets. As the analysis of the original paper intends to be systematic, it is important to observe the effect of a more recent version of the interactome on the results and their significance. We found that the results of the paper, while being reproducible, are affected by the use of a more recent interactome, mainly on the number of significant results.

## 1 Introduction

An interactome is a graph containing all the biologically relevant molecular interactions found within a cell. This notion first appeared in 1999 for the drosophila (Sanchez et al., 1999) and the need to thoroughly study this structure has been expressed less than 15 years ago (Barabasi and Oltvai, 2004).

The interactome is one of many biological networks. Among others, we can find the genome, covering gene networks, the proteome for the protein networks (Rolland et al., 2014), disease networks (Goh et al., 2007). Biological networks provide the ability to deeply study biology (Barabasi and Oltvai, 2004), as well as medicine (Barabási et al., 2011) and, more recently, pharmacology (Hopkins, 2008).

Diseases are considered as the result of an interplay between molecular interactions. The need to use the interactome as a tool to analyze genetic diseases behaviour had already been expressed several years ago (Vidal et al., 2011). However, the interactome is incomplete and estimated around 20%-complete for the interactions involved and around 54%-complete for the proteins involved (Amaral, 2008; Stumpf et al., 2008). The authors of the original paper (Menche et al., 2015) showed that the human interactome has now reached sufficient completion to systematically study diseases. Moreover, the interactome now allows the study of many more genetic relations, such as

drug-disease correlation (Yu et al., 2016) or digenic diseases (Gazzo et al., 2015).

In the original paper, authors extracted genes associated with diseases from several disease genes association databases, in particular OMIM, the Online Mendelian Inheritance in Man (Amberger et al., 2008), and GWAS, the Genome-Wide Association Studies, compiled by PhenGenI (Ramos et al., 2014). These genes were mapped on the human interactome in order to determine the properties of these disease modules in the graph. They discovered firstly that diseases tend to *cluster* in denser subgraphs than the interactome itself and secondly that phenotypically close diseases tend to overlap on a significant amount of genes.

The first part of this paper focuses on the reproduction of some of the results of the original paper, namely the disease modules propensity to cluster into highly connected components and the significantly lower separation indicator values for highly gene related disease pairs. The second part will reproduce the results with an updated interactome in order to test the robustness of the analysis. In the third part, we will discuss an analytical way of determining simulations results.

## 2 Results

### 2.1 Reproducibility

The interactome used in the original paper contains 13,460 genes and 141,296 physical interactions constructed on several interactions databases including BioGRID (Chatr-aryamontri et al., 2017), IntAct (Kerrien et al., 2011), TRANSFAC (Matys et al., 2003), MINT (Licata et al., 2011), HPRD (Keshava Prasad et al., 2008), KEGG and BIGG (Lee et al., 2008), CORUM (Ruepp et al., 2009) and PhosphitePlus (Hornbeck et al., 2011).

Authors chose to rely only on physical protein-protein interactions (PPI) and to exclude functional interactions (Caldera et al., 2017). This interactome is available for download in the supplementary material.

The diseases studied are selected such that they possess at least 20 genes associated to them. We obtained 29,775 disease-gene associations on 3,173 distinct genes,

with 2,436 genes found in the interactome.

**Clustering of disease modules** The original paper discusses the tendency of the diseases to cluster into dense subgraphs. In order to check this hypothesis, we analyzed the largest connected component (LCC) of the diseases in the interactome. We compared the relative size of the module, defined by  $r = S/N_d$ , with  $S$  the size of the LCC of the disease, and  $N_d$ , the number of genes associated with the given disease, with the  $z$ -score of the LCC size of a disease, which is computed by comparing the relative size of the module with the size of the largest LCC of the disease obtained by chance (Figure 1).

We observed that 241 out of the 299 diseases (more than 80%) have a significantly bigger LCC than expected by chance. The  $z$ -score of the LCC size of a disease is strongly related to its relative module size.

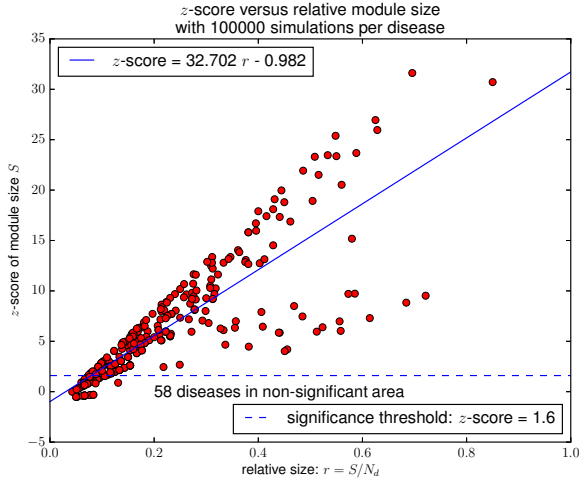


**Figure 1:  $z$ -score of largest connected component size vs relative module size.** 100,000 simulations have been performed per disease in order to determine the size of the largest connected component of the disease subgraph expected by chance. Diseases being highly connected, thus highly covered by the interactome, present a higher  $z$ -score and then a higher confidence about the significance of the clustering observed. Assuming that the distribution of largest connected component is normal for random samples (Barraez et al., 2000), each  $z$ -score can be associated to a  $p$ -value, in particular,  $z\text{-score} \geq 1.6$  corresponds to  $p\text{-value} \leq 0.05$ , representing significance threshold (dotted line in the plot).

We observed that several diseases do not present a significantly larger largest connected component than expected by chance. These diseases have a small relative size, less than 20% of their related genes are connected in the current interactome. On the other hand, diseases with bigger relative size have a higher  $z$ -score, leading us to think that a more complete interactome, with higher coverage of the diseases could increase the significance of the result.

These results confirm the observation of the original paper that disease modules tend to cluster.

**Separation distribution** The original paper describes the separation of diseases in the interactome through

$J = 0$	$0 < J < 1$	$J < 1$	$J = 1$
$C = 0$	$0 < C < 1$	$C = 1$	$C = 1$
No common gene	Partial overlap	$A$ is complete subset of $B$	$A$ and $B$ are identical

**Table 1:** Meaning of the different  $J$ -score/ $C$ -score combinations.

two different measures. The first one is the overlapping scores,  $C$ -score and  $J$ -score, defined respectively as  $|A \cap B| / \min(|A|, |B|)$  and  $|A \cap B| / |A \cup B|$  for  $A$  and  $B$  two disease genes sets. The second one is the separation score,  $s_{AB}$ , defined as follows :

$$s_{AB} = \langle d_{AB} \rangle - \frac{\langle d_A \rangle + \langle d_B \rangle}{2}. \quad (1)$$

for two diseases  $A$  and  $B$ , with  $\langle d_A \rangle$  and  $\langle d_B \rangle$  as the mean distance between two proteins in the disease subgraphs of  $A$  and  $B$  respectively, and with  $\langle d_{AB} \rangle$  as the mean distance between two proteins of each disease subgraph.

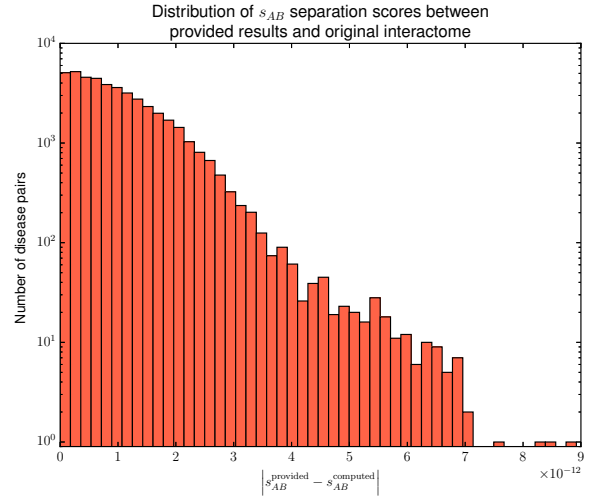


**Figure 2: Distribution of the difference between the provided  $s_{AB}$  score and the computed  $s_{AB}$  score.** We observe that difference is very small, below  $10^{-11}$ , which can be ascribed to computation precision.

We analyzed the distribution of the number of disease pairs separated into different groups according to the combination of their overlapping scores (Table 1) according to their separation score (Figure 3). We found similar results to the ones in the original paper, with the fact that diseases sharing no common genes are also mainly separated ( $s_{AB} > 0$ ), even though some modules overlap. However, complete overlap of the modules showed a great diversity of separating scores. The only difference observed was that for non-overlapping disease pairs, the amount of pairs having a separation value below 0 is 710 versus 717 in the original paper, which is due to computation precision since all computed separation values deviate by less than  $10^{-11}$  from provided values by authors of the original paper (Figure 2).

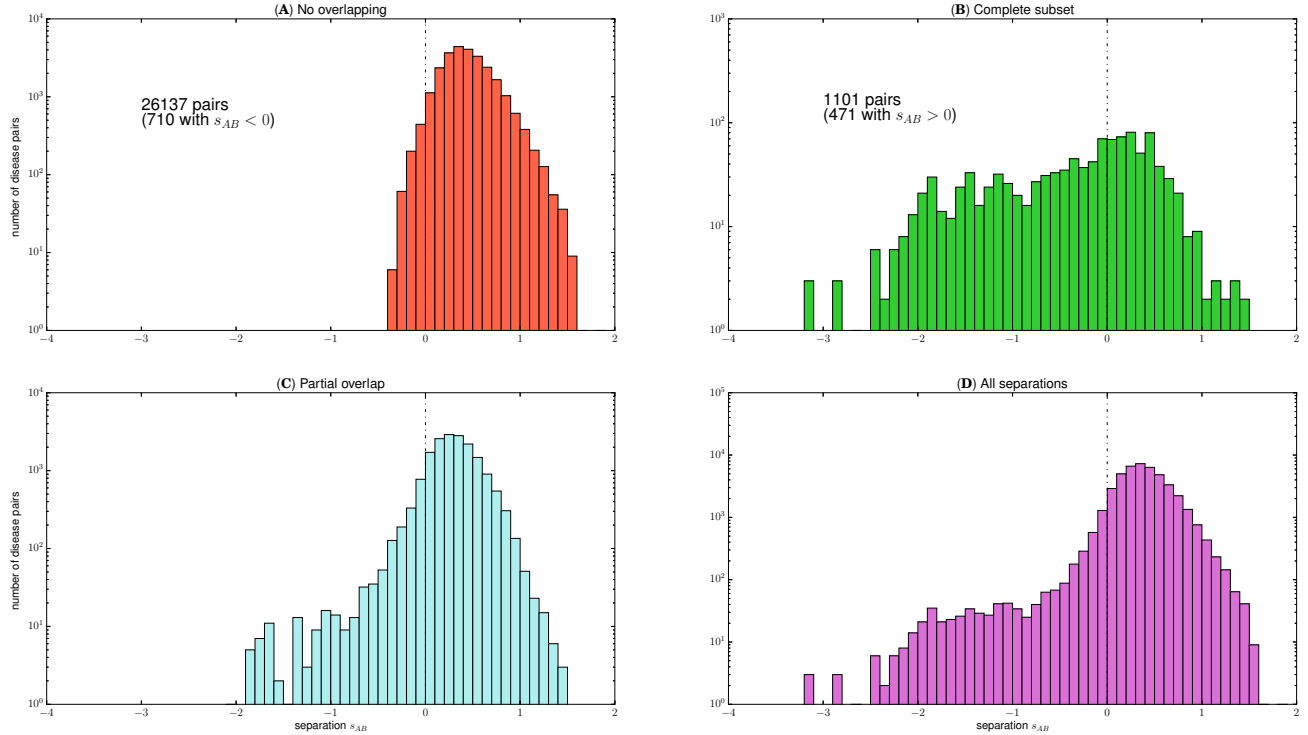


**Figure 3: Disease pairs separation.** (A) The  $s_{AB}$  distribution of disease pairs with no common gene ( $C$ -score =  $J$ -score = 0). We observe that even though no gene is shared, 710 of the 26,137 pairs (less than 3%) have a negative separation score (between 0 and 0.5). (B) The  $s_{AB}$  distribution of disease pairs with complete overlap ( $J$ -score <  $C$ -score = 1). We observe that despite the inclusion of one disease genes set in the other, 471 of the 1,101 pairs (more than 42%) have a positive separation score. Yet, separation goes to very low values (below 2). (C) The  $s_{AB}$  distribution of disease pairs partially overlapping ( $0 < J$ -score  $\leq C$ -score < 1). These disease pairs show the same spike of frequency right to  $s_{AB} = 0$  as in (A) and the same tail of frequency left to  $s_{AB} = 0$ . (D) The  $s_{AB}$  distribution of all the disease pairs.

## 2.2 Robustness

We wanted to check if the results of the original paper will still hold with a more recent interactome. To reach this aim, we obtained an updated interactome and reproduced the previous analyses with the new dataset.

**Databases update** The newer version of the interactome yields a new graph having 17,786 nodes and 370,326 edges, a bit more than 1.3 times the initial amount of nodes, and more than 2.6 times the initial amount of edges of the original interactome used. From the 4,326 genes added in this newer version, 361 are associated with at least one of the 299 diseases, leading to 2,797 disease-associated genes in the interactome. This reduces the proportion of disease-associated genes of the interactome from 18% in the original version to less than 16% in the newer one.

This newer version contains then around 71% of the estimated number of proteins and 57% of the estimated interactions of the interactome (Amaral, 2008; Stumpf et al., 2008).

Disease genes considered in this update are the same 299 diseases studied in the original paper. Further investigation could include also an update of the disease list.

## 2.3 Comparison with original results

By defining the density of a graph  $\Gamma = (V, E)$  as being  $d(\Gamma) := |E| / \binom{|V|}{2}$ , we find that the newer interactome is more than 1.5 times denser than the original one with 0.156% versus 0.234% for the newer one.

**Clustering of disease modules** We performed the same analysis as previously to study the clustering of the disease modules in the interactome with the new version (Figure 4). We observed that 12 more diseases have a  $z$ -score below the significance threshold compared to the previous results. We also noted a general decrease of the  $z$ -score.

In order to understand the origin of this decrease in the  $z$ -score, we compared the relative size distribution of the disease modules of the original and the new interactome (Figure 5). We noted that the relative size has shifted towards right.

This can be explained by the increase of the number of genes, leading to a higher coverage of the disease modules, and the increase of the number of interaction, leading to a more connected interactome and therefore disease modules potentially more connected. Although, the maximum  $z$ -score has dropped from 31.6 to 27.5, the mean  $z$ -score has increased from 6.2 to 6.4 due in part to the increase of the

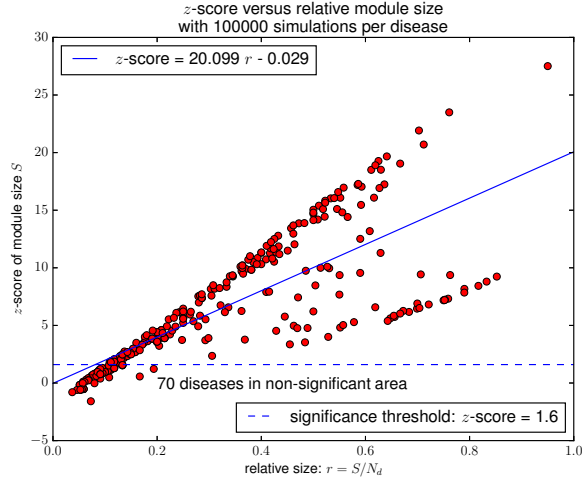


**Figure 4: z-score of the largest connected component size vs relative module size of the newer interactome.** Adaptation of Figure 1 on the new version of the interactome.

number of disease modules with a  $z$ -score  $\in [10, 20]$ .

Another observation was that the average relative size for the given diseases has increased from 22% to 32% in the new interactome, demonstrating the better coverage brought by the updated version.

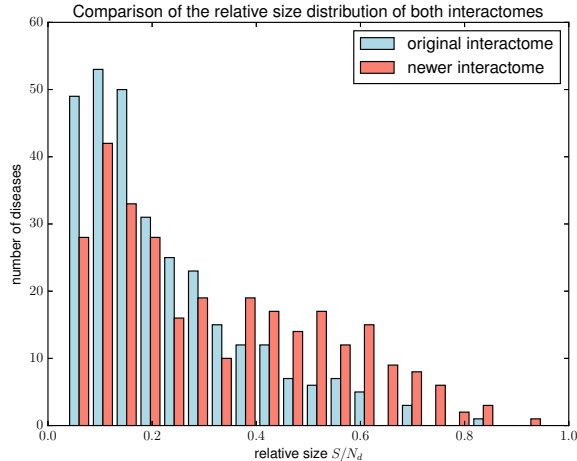


**Figure 5: Comparison of relative size distribution between original and newer interactomes.** We observe that the number of diseases having a relative size below  $\simeq 0.35$  has lowered, whereas the number of diseases having a relative size above  $\simeq 0.35$  has increased. This is explained by the bigger density of the new interactome, leading to larger LCC in the disease subgraphs.

The interpretation of Subsection 2.1 still stand: diseases having a low  $z$ -score still have a low relative size, and diseases with a higher  $z$ -score have a higher relative size. So either the interactome is still too incomplete for these diseases, or they lie in very sparse regions of the interactome. A further investigation of these diseases and their genes is needed to better understand this phenomenon. Due to the

graph density increase, the degree distribution has changed as well (Figure 6).

The networks are scale-free, and its degree distribution still follows a power law, which is inherent to biological networks. A power law is characterized by a few nodes being highly connected to the other ones, whereas most nodes are connected to only a few other ones. We approximated the distribution with a linear regression following the relation  $\log(P(k)) \sim -\gamma \log(k)$  and determined the  $\gamma$  coefficients for each distribution. The new interactome has a coefficient of 1.6 while the original one has a coefficient of 1.53. The  $\gamma$  coefficients are bigger than 1 and smaller than 3, which is considered standard for biological networks (Barabasi and Oltvai, 2004; Vidal et al., 2011). This result means that while both the original interactome and the new one are highly alike and comparable on their degree distribution, the difference is that the new interactome contains more highly connected nodes, with a mean twice as big.

So the decrease of the  $z$ -score below the threshold of these 12 diseases is also due to the increase of the interactome density. The increase in the interactome density implies that a subgraph taken at random tends to have a wider LCC at equal size, which is then used for the computation of the  $z$ -scores.

**Separation distribution** When analyzing the separation distribution of the different subgroups of the diseases modules pairs with the new interactome (Figure 7), we observed that non-overlapping diseases have a higher separation score. With the original interaction, we had 710 disease pairs with a negative separation, whereas with the new interactome we observed only 324 pairs with  $s_{AB} > 0$  score, meaning that 54% of the non-overlapping disease pairs increased their separation score above 0.

We also observe that 6% of the complete subset disease pairs decreased their separation score below 0, however this result is less significant as we observed a large diversity of separation scores for this category.

When we looked at all the disease pairs together, we observed that separation scores have tightened around 0:  $s_{AB}$  is in  $[-3.2, 1.6]$  in the original interactome, and in the new one,  $s_{AB}$  is in  $[-2.5, 1.1]$ .

### 3 Extension of the subgraph largest connected component distribution

The computation of the  $z$ -scores require a null hypothesis. We used here the random hypothesis. The  $z$ -scores are computed as follows: if  $S_D$  is the disease module associated with a given disease  $D$ , then its  $z$ -score is given by:

$$z\text{-score} = \frac{|S_D| - \mu(S^{\text{rand}})}{\sigma(S^{\text{rand}})}, \quad (2)$$

with  $\mu(S^{\text{rand}})$  and  $\sigma(S^{\text{rand}})$  being respectively the mean and the standard deviation of the largest connected component

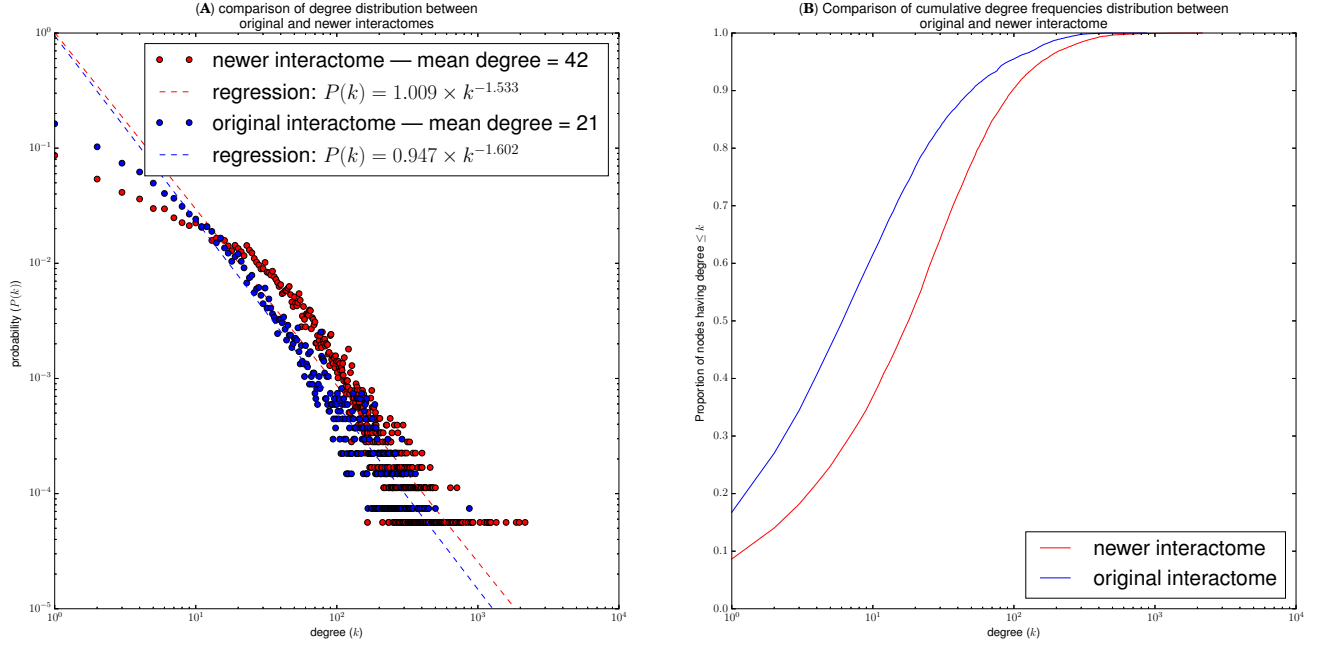


**Figure 6: Degree distribution comparison.** (A) Both the original interactome and the new one are scale-free, i.e. their degree distribution follows a power law. The power law can be approximated with a linear regression according to the relation  $\log(P(k)) \sim -\gamma \log(k)$ . The new interactome has a smaller  $\gamma$  coefficient, meaning that a bigger proportion of nodes have a high degree, compared to the original one. (B) Cumulative degree distribution of both the original and the newer interactome. We observe easily the power law characteristic that even though degree can reach 2,000, almost all the interactome nodes have a degree  $\leq 100$ .

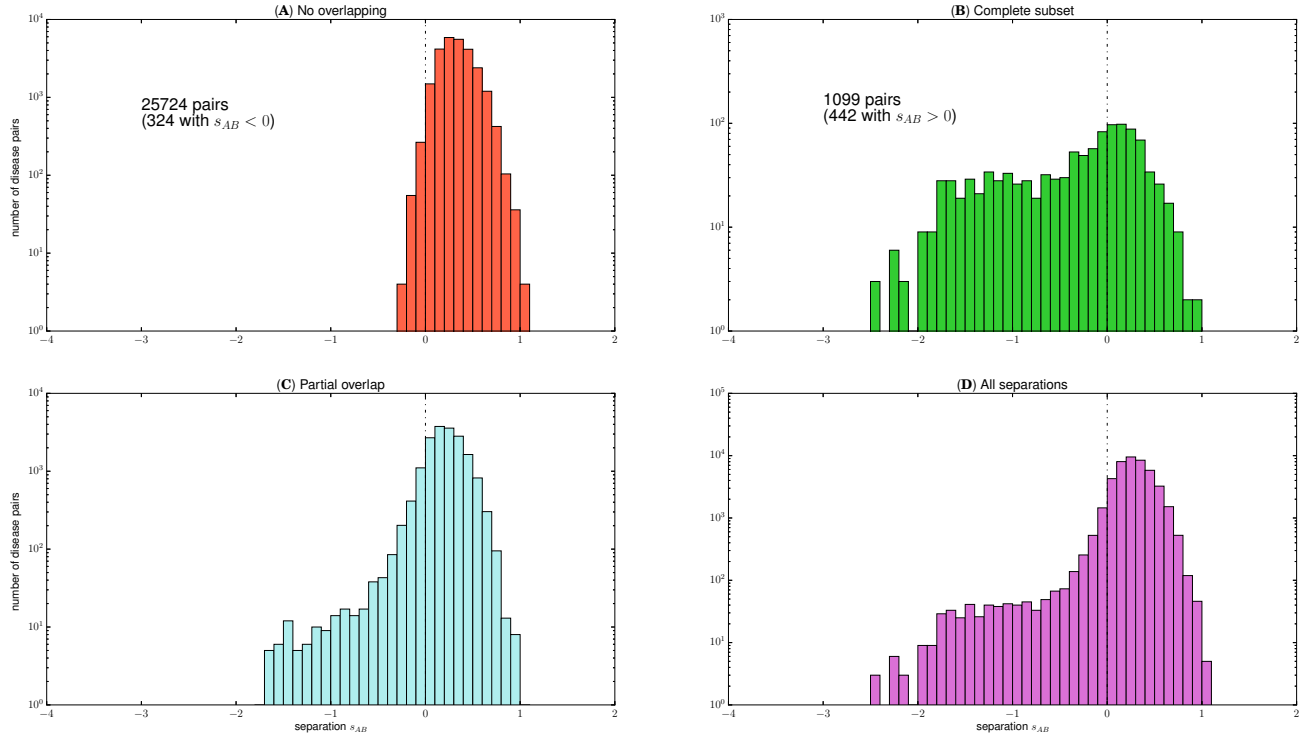


**Figure 7: Disease pairs separation in the new interactome.** Adaptation of Figure 3 with the updated interactome. (A) We observe that more than half of the disease pairs sharing no genes that had a negative  $s_{AB}$  score in the original interactome now have a positive score, due to a decrease in  $\langle d_A \rangle$  and  $\langle d_B \rangle$  because of the higher density of the newer interactome. (B) We also observe that 29 disease pairs related by inclusion had a score right shift towards positive values.



size of a random subgraph of size  $|D|$  in the interactome.

These values are obtained by simulations: taking subgraphs at random of given size in the interactome yields a distribution  $P(S^{\text{rand}})$  with a given mean  $\mu(S^{\text{rand}})$  and standard deviation  $\sigma(S^{\text{rand}})$  (Figure 8).

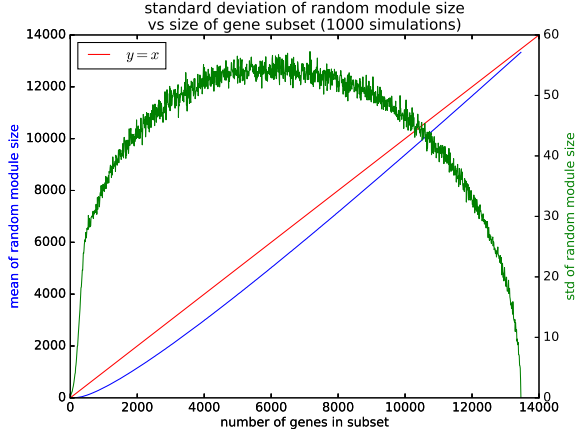


**Figure 8:**  $S^{\text{rand}}$  mean and standard deviation distribution of the original interactome. With  $10^3$  simulations per subgraph size, we obtain the distribution of the largest connected component size in the interactome. We observe that for subsets of small size  $k$ , the expected LCC size is significantly smaller than  $k$  whereas for subsets of big size  $K$  (giant components), the expected LCC size is much closer to  $K$ .

In order to avoid simulation computation time, we decided to analytically determined probability density with a probability mass function. For a graph  $\Gamma = (V, E)$  such that  $|E| = m$  and  $\Lambda_k^m(V, \cdot)$ , the set of all graphs having  $V$  as vertex set,  $m$  edges, and a LCC of size  $k$ , we define  $p_k$ , the probability that  $\Gamma$  has LCC of size  $k$  as:

$$p_k = \frac{|\Lambda_k^m(V, \cdot)|}{\binom{|V|}{2}^m}, \quad (3)$$

which requires  $|\Lambda_k^m(V, \cdot)|$  to be computed. However, this set cardinality is defined by a recurrence relation (see proof in supplementary materials), which makes computations several orders of magnitude slower, even with dynamic programming and caching, meaning that the time gained by not repeating the simulation is lost because of the computation time required for the analytical computation.

A Python3 implementation is given in `source/lcc_size/`.

## 4 Conclusion

## 5 Materials and Methods

### 5.1 Network analysis

The newer version of the interactome and the source code for all plots presented here as well as this very paper are available at the following web page: <https://github.com/RobinPetit/INFOF-308>.

### 5.2 Database update

In order to update the interactome, the tool *inter-tool* (Catabia et al., 2017) has been used. Inter-build (one of the programs from Inter-tools) requires datasets in the PSI-MITAB format, an extension of the PSI-MI format (Kerrien et al., 2007), and outputs a tsv file.

The outputted file by Inter-build and the interactome provided with the original paper both use Entrez gene IDs, they can therefore easily be merged. In order to merge these, the script `merger.py` has been written. As these two tsv files have a different format (different columns), only the gene IDs are outputted by `merger.py`.

Latest datasets from BioGRID, IntACT, and the Database of Interacting Proteins (DIP) (Salwinski et al., 2004) (July 25th) and of MINT (July 27th) have been downloaded and merged. The resulting interactome was merged with the original one in order to add the interactions to the previous version.

The others databases cited in Subsection 2.1 were not included in the newer interactome because they were not available for download in a Inter-build-compatible format.

## References

- Amaral, L. A. N. (2008). A truer measure of our ignorance. *Proceedings of the National Academy of Sciences*, 105(19):6795–6796.
- Amberger, J., Bocchini, C. A., Scott, A. F., and Hamosh, A. (2008). McKusick’s online mendelian inheritance in man (omim®). *Nucleic acids research*, 37(suppl.1):D793–D796.
- Barabási, A.-L., Gulbahce, N., and Loscalzo, J. (2011). Network medicine: a network-based approach to human disease. *Nature reviews. Genetics*, 12(1):56.
- Barabasi, A.-L. and Oltvai, Z. N. (2004). Network biology: understanding the cell’s functional organization. *Nature reviews. Genetics*, 5(2):101.
- Barraez, D., Boucheron, S., and Fernandez De LaVega, W. (2000). On the fluctuations of the giant component. *Comb. Probab. Comput.*, 9(4):287–304.
- Caldera, M., Buphamalai, P., Müller, F., and Menche, J. (2017). Interactome-based approaches to human disease. *Current Opinion in Systems Biology*.
- Catabia, H., Smith, C., and Ordovás, J. (2017). Inter-tools: a toolkit for interactome research.
- Chatr-aryamontri, A., Oughtred, R., Boucher, L., Rust, J., Chang, C., Kolas, N. K., O’Donnell, L., Oster, S., Theesfeld, C., Selam, A., et al. (2017). The biogrid interaction database: 2017 update. *Nucleic acids research*, 45(D1):D369–D379.
- Gazzo, A. M., Daneels, D., Cilia, E., Bonduelle, M., Abramowicz, M., Van Dooren, S., Smits, G., and Lenaerts, T. (2015). Dida: A curated and annotated digenic diseases database. *Nucleic acids research*, 44(D1):D900–D907.

- Goh, K.-I., Cusick, M. E., Valle, D., Childs, B., Vidal, M., and Barabási, A.-L. (2007). The human disease network. *Proceedings of the National Academy of Sciences*, 104(21):8685–8690.
- Hopkins, A. L. (2008). Network pharmacology: the next paradigm in drug discovery. *Nature chemical biology*, 4(11):682–690.
- Hornbeck, P. V., Kornhauser, J. M., Tkachev, S., Zhang, B., Skrzypek, E., Murray, B., Latham, V., and Sullivan, M. (2011). Phosphositeplus: a comprehensive resource for investigating the structure and function of experimentally determined post-translational modifications in man and mouse. *Nucleic acids research*, 40(D1):D261–D270.
- Kerrien, S., Aranda, B., Breuza, L., Bridge, A., Broackes-Carter, F., Chen, C., Duesbury, M., Dumousseau, M., Feuermann, M., Hinz, U., et al. (2011). The intact molecular interaction database in 2012. *Nucleic acids research*, 40(D1):D841–D846.
- Kerrien, S., Orchard, S., Montecchi-Palazzi, L., Aranda, B., Quinn, A. F., Vinod, N., Bader, G. D., Xenarios, I., Wojcik, J., Sherman, D., et al. (2007). Broadening the horizon—level 2.5 of the hupo-psi format for molecular interactions. *BMC biology*, 5(1):44.
- Keshava Prasad, T., Goel, R., Kandasamy, K., Keerthikumar, S., Kumar, S., Mathivanan, S., Telikicherla, D., Raju, R., Shafreen, B., Venugopal, A., et al. (2008). Human protein reference database—2009 update. *Nucleic acids research*, 37(suppl\_1):D767–D772.
- Lee, D.-S., Park, J., Kay, K., Christakis, N., Oltvai, Z., and Barabási, A.-L. (2008). The implications of human metabolic network topology for disease comorbidity. *Proceedings of the National Academy of Sciences*, 105(29):9880–9885.
- Licata, L., Briganti, L., Peluso, D., Perfetto, L., Iannuccelli, M., Galeota, E., Sacco, F., Palma, A., Nardoza, A. P., Santonico, E., et al. (2011). Mint, the molecular interaction database: 2012 update. *Nucleic acids research*, 40(D1):D857–D861.
- Matys, V., Fricke, E., Geffers, R., Gößling, E., Haubrock, M., Hehl, R., Hornischer, K., Karas, D., Kel, A. E., Kel-Margoulis, O. V., et al. (2003). Transfac®: transcriptional regulation, from patterns to profiles. *Nucleic acids research*, 31(1):374–378.
- Menche, J., Sharma, A., Kitsak, M., Ghiassian, S. D., Vidal, M., Loscalzo, J., and Barabási, A.-L. (2015). Uncovering disease-disease relationships through the incomplete interactome. *Science*, 347(6224).
- Ramos, E. M., Hoffman, D., Junkins, H. A., Maglott, D., Phan, L., Sherry, S. T., Feolo, M., and Hindorff, L. A. (2014). Phenotype-genotype integrator (phegeni): synthesizing genome-wide association study (gwas) data with existing genomic resources. *European Journal of Human Genetics*, 22(1):144.
- Rolland, T., Taşan, M., Charlotiaux, B., Pevzner, S. J., Zhong, Q., Sahni, N., Yi, S., Lemmens, I., Fontanillo, C., Mosca, R., et al. (2014). A proteome-scale map of the human interactome network. *Cell*, 159(5):1212–1226.
- Ruepp, A., Waegele, B., Lechner, M., Brauner, B., Dunger-Kaltenbach, I., Fobo, G., Frishman, G., Montrone, C., and Mewes, H.-W. (2009). Corum: the comprehensive resource of mammalian protein complexes—2009. *Nucleic acids research*, 38(suppl\_1):D497–D501.
- Salwinski, L., Miller, C. S., Smith, A. J., Pettit, F. K., Bowie, J. U., and Eisenberg, D. (2004). The database of interacting proteins: 2004 update. *Nucleic acids research*, 32(suppl\_1):D449–D451.
- Sanchez, C., Lachaize, C., Janody, F., Bellon, B., Röder, L., Euzenat, J., Rechenmann, F., and Jacq, B. (1999). Grasping at molecular interactions and genetic networks in drosophila melanogaster using flynets, an internet database. *Nucleic acids research*, 27(1):89–94.
- Stumpf, M. P., Thorne, T., de Silva, E., Stewart, R., An, H. J., Lappe, M., and Wiuf, C. (2008). Estimating the size of the human interactome. *Proceedings of the National Academy of Sciences*, 105(19):6959–6964.
- Vidal, M., Cusick, M. E., and Barabási, A.-L. (2011). Interactome networks and human disease. *Cell*, 144(6):986–998.
- Yu, L., Wang, B., Ma, X., and Gao, L. (2016). The extraction of drug-disease correlations based on module distance in incomplete human interactome. *BMC systems biology*, 10(4):111.